Journal of Engineering Sciences, Assiut University, Vol. 40, No. 5, pp.1411-1433 - September 2012.

VOLTAGE STABILITY ENHANCEMENT USING FACTS DEVICES

Prof. Gaber El-Saady[1], Prof. Mohamed A. A. Wahab[2] , Dr. Mohamed M. Hamada[2] and M. F. Basheer[3]

[1] *Faculty of Engineering, Assiut University ,*
[2] *Faculty of Engineering, El-Minia University*
[3] *Ministry of Electricity and Energy.*

(Received December 21, 2011 Accepted July14, 2012)

The aim of this paper is to investigate the enhancement of a steady state voltage stability via shunt and series FACTS devices namely, static synchronous compensator (STATCOM) and static synchronous series compensator (SSSC). In order to select the best locations of FACTS devices, a modal analysis is used to determine the weakest bus of the studied system, while the voltage stability proximity index under line outage contingencies is used to identify the critical lines. The analysis is preformed on IEEE 30 bus system. The proposed schemes are tested under different loading conditions. The simulation results demonstrate the feasibility and effectiveness of the proposed devices. Also, the results obtained allow concluding that the STATCOM shunt device improves the voltage stability margin better than the SSSC series device.

1. INTRODUCTION

Structural changes in the electrical sector, such as those caused by privatization and deregulation, modification of the network topology, as well as ever increasing in load demands brought by economic and environmental pressures that led the power systems to operate near its stability limits, increase the utilities interest about the voltage instability and voltage collapse problems.

A large number of researchers have been interested in the voltage stability problem. Their attention has resulted with a numerous number of papers, books, and reports being published. Most of these are reported in the extensive bibliography [1].

Generally, voltage collapse is the process by which the sequence of events accompanying voltage instability leads to a low unacceptable voltage profile in a significant part of the power system.

Voltage collapse may be a possible outcome of voltage instability, which is defined as the attempt of load dynamics to restore power consumption beyond the capability of the combined transmission and generation system [2].

The voltage instability may be classified into transient and steady state, the latest is the most common reason for voltage collapse. Steady state voltage stability or Small-disturbance voltage stability refers to the system's ability to maintain steady voltages when subjected to small perturbations such as incremental changes in system load [3].

Many of measures used to prevent voltage instability [4] such as, (i). Placement of series and shunt capacitors, ii. Generation rescheduling, iii. Placement of FACTS controllers, iv. Under-Voltage load shedding, v. Blocking of Tap-Changer under reverse operation, vi. Installation of synchronous condensers.

There are many types of FACTS used to enhance voltage stability such as, Superconducting magnetic energy storage (SMES) [5], Static Var Compensator (SVC) [6], Static Synchronous Compensator (STATCOM) [7], Static Synchronous Series Compensator (SSSC) [8], Thyristor Controlled Series Capacitor (TCSC) [9], Interline Power Flow Controller (IPFC) [10], and Unified Power Flow controller (UPFC) [11]. Also some comparative study has been published as the comparison between SVC, STATCOM, TCSC, and UPFC [12][13].

The rest of this paper is structured as follows. In section 2, the concept of the steady state voltage stability model is introduced. In section 3 the proposed methodologies for the best placement of FACTS are considered. The detailed static voltage stability model of STATCOM and SSSC has been explained in section 4. The results obtained for the test system is given and discussed in Section 5. Finally, Section 6 contains the conclusion.

2. STEADY STATE VOLTAGE STABILITY

The steady state (or static) analysis mainly depends on the steady state models, such as power flow model or a linearized dynamic model described by the steady state operation. These methods [14-16] can be divided into:

1. Load flow feasibility methods, which depend on the existence of an acceptable voltage profile across the network. This approach is concerned with the maximum power transfer capability of the network or the existence of a solved load flow case. There are many criteria proposed under this approach. Some of these criteria are the following:
   - The reactive power capability (Q-V curve).
   - Maximum power transfer limit (P-V curve).
   - Voltage stability proximity index (VSI) or the load flow feasibility index (LFF index).
2. Steady state stability methods, which test the existence of a stable equilibrium operating point of the power system. Some of the criteria proposed under this approach are:
   - Eigenvalues of linearized dynamic equations.
   - Singular value of Jacobian matrix (SVJ).
   - Sensitivity matrices.

In this paper the two FACTS devices are used, one is shunt device (STATCOM) and the other is series type (SSSC). To select the best location for these devices, two different suitable algorithms are used. As the shunt devices affect mainly on the bus, the weakest bus is identified as a best location for such device using Modal analysis. While the critical line lead to voltage instability is investigated to select the best location for the series device. For each procedure the power flow is the first step.

Power Flow Model for Voltage Stability Analysis

The power flow model is used to study steady state voltage stability since the power flow equation yields adequate results, as singularities in related power flow Jacobian can be associated with actual singular bifurcation of the corresponding dynamical system [17]. The power flow model is represented by:

$$F(x,\lambda)=\begin{bmatrix}\Delta P(x,\lambda)\\ \Delta Q(x,\lambda)\end{bmatrix}=0 \qquad (1)$$

where $F(x,\lambda)$ is power flow equation and λ is Loading Factor (LF) or system load change that drives the system to collapse in the following way:

$$P_{D,i}=P_{Do,i}(1+\lambda K_{P,i})$$
$$Q_{D,i}=Q_{Do,i}(1+\lambda K_{Q,i}) \qquad (2)$$

where $P_{Do,i}$ and $Q_{Do,i}$ represent the initial active and reactive loads at bus i and constants K_{Pi} and K_{Qi} represent the active and reactive load increase direction of bus i respectively.

3. BEST PLACEMENT OF FACTS DEVICES FOR VOLTAGE STABILITY ENHANCEMENT

To determine the best location of proposed FACTS devices, There are different techniques are utilized. The following sections describe the proposed methods.

3.1 Identifying Weakest Bus for Best STATCOM Location Using Modal Analysis Method :

Modal or Eigenvalue Analysis Method can predict voltage collapse in complex power system networks. It involves mainly the computing of the smallest eigenvalues and associated eigenvectors of the reduced Jacobian matrix obtained from the load flow solution. the participation factor can be used effectively to find out the weakest nodes or buses in the system [18].

The Newton-Raphson power flow equation represented by:

$$\begin{bmatrix}\Delta P\\ \Delta Q\end{bmatrix}=\begin{bmatrix}J_{11} & J_{12}\\ J_{21} & J_{22}\end{bmatrix}\begin{bmatrix}\Delta\theta\\ \Delta V\end{bmatrix}=J\begin{bmatrix}\Delta\theta\\ \Delta V\end{bmatrix} \qquad (3)$$

In order to focus the study of the reactive demand and supply problem of the system as well as minimize computational effort by reducing dimensions of the Jacobian matrix J the real power via putting, $\Delta P=0$ in Equation (3):

$$\Delta P=0=J_{11}\Delta\theta+J_{12}\Delta V \quad , \quad \Delta\theta=-J_{11}^{-1}J_{12}\Delta V \qquad (4)$$

and

$$\Delta Q = J_{21}\Delta\theta + J_{22}\Delta V \qquad (5)$$

From equations (4) and (5) :

$$\Delta Q = J_R \Delta V = [J_{22} - J_{21}J_{11}^{-1}J_{12}]\Delta V \qquad (6)$$

where J_R is the reduced Jacobian matrix of the system.

The eigenvalues and eigenvectors of the reduced order Jacobian matrix J_R are used for the voltage stability characteristics analysis. To detect voltage instability, modes of the eigenvalues matrix J_R is identified. The magnitude of the eigenvalues provides a relative measure of proximity to instability.

Eigenvalue analysis of J_R will be as follows:

$$J_R = \Phi\Lambda\Gamma \qquad (7)$$

where ,

Φ = right eigenvector matrix of J_R

Γ = left eigenvector matrix of J_R

Λ =diagonal eigenvalue matrix of J_R

and $\Phi\Gamma = 1$

Equation (7) may be written as:

$$J_R^{-1} = \Phi\Lambda^{-1}\Gamma \qquad (8)$$

From Equations (8) and (6):

$\Delta V = \Phi\Lambda^{-1}\Gamma\Delta Q$, or

$$\Delta V = \sum_i \frac{\Phi_i \Gamma_i}{\lambda_i}\Delta Q \qquad (9)$$

where λ_i is the i^{th} eigenvalue, Φ_i is the i^{th} column right eigenvector and Γ_i is the i^{th} row left eigenvector of matrix J_R .

Each eigenvalue λ_i and corresponding right and left eigenvectors Φ_i and Γ_i , define the i^{th} mode of the system. The i^{th} modal reactive power variation is defined as:

$$\Delta Q_{mi} = K_i \Phi_i \qquad (10)$$

Wkere K_i is a scale factor to normalize vector ΔQ_i so that :

$$K_i^2 \sum_j \Phi_{ji}^2 = 1 \qquad (11)$$

with Φ_{ji} the j^{th} element of Φ_i

The corresponding i^{th} modal voltage variation is :

$$\Delta V_{mi} = \frac{1}{\lambda_i} \Delta Q_{mi} \qquad (12)$$

Equation (12) indicates that if all the eigenvalues are positive, J_R is positive definite and the V-Q sensitivities are also positive, and the system is voltage stable [19]. The system is considered voltage unstable if at least one of the eigenvalues is negative. A zero eigenvalue of J_R means that the system is close to voltage instability. Furthermore, small eigenvalues of J_R determine the proximity of the system to being voltage unstable. So, once the minimum eigenvalues and the corresponding left and right eigenvectors have been calculated, the participation factor can be used to identify the weakest node or bus in the system.

The procedure may be summarized as follows:

- Obtain the load flow for the base case of the system and get the jacobian matrix (J) and the reduced jacobian (J_R)
- Compute the eigenvalues to identify how the system close to instability and find the minimum eigenvalue ($\lambda_{\min}$) of J_R .
- Calculate the right and left eigenvectors of J_R and compute the participation factors P_{ki} for $(\lambda_{\min})_i$. The highest P_{ki} indicates the most participated k^{th} bus to i^{th} mode (which is the closest mode to instability) in the system.
- Generate the Q-V curve to the k^{th} bus. By using Q-V curves, it is possible to know what is the maximum reactive power that can be achieved or added to the weakest bus before reaching minimum voltage limit or voltage instability

3.2 Line Outage Contingency Analysis for Best SSSC Location

Voltage stability index under different line outage contingencies is used to select the appropriate location for SSSC, This is done by simulating the line outage in the power flow procedure.

When a line outage occurs the jacobian matrix needs to be modified to reflect the outage effect [20]. To make such modification a nominal π circuit of an outage line *i-j* is presented in Fig. (1). The two power injections S_{ci} and S_{cj} represent the effect of the outage [21].

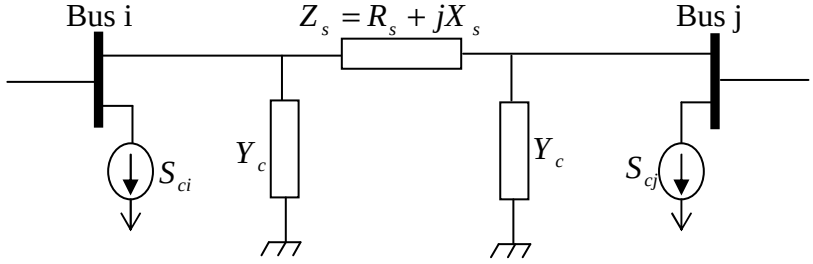

Fig. 1: Power injection model for line *i-j*

To simplify the derivation let

$$Y_s = \frac{1}{Z_s} = |Y_s| e^{-j\delta s}$$

The outage effect is simulated by making the two power injection S_{ci} and S_{cj} equal to the power flows on the outgae line with opposite signs. Therefore :

$$\begin{aligned} S_{ci} &= jY_C V_i^2 - V_i^2 |Y_S| e^{j\delta_s} + V_i V_j |Y_S| e^{j(\delta_s + \theta_i - \theta_j)} \\ &= P_{ci} + jQ_{ci} \end{aligned} \quad (13)$$

$$\begin{aligned} S_{cj} &= jY_C V_j^2 - V_j^2 |Y_S| e^{j\delta_s} + V_i V_j |Y_S| e^{j(\delta_s + \theta_j - \theta_i)} \\ &= P_{cj} + jQ_{cj} \end{aligned} \quad (14)$$

$$P_{ci} = V_i V_j |Y_S| \cos(\delta_s + \theta_i - \theta_j) - V_i^2 |Y_S| \cos\delta_s \quad (15)$$

$$Q_{ci} = V_i V_j |Y_S| \sin(\delta_s + \theta_i - \theta_j) - V_i^2 |Y_S| \sin\delta_s + Y_C V_i^2 \quad (16)$$

$$P_{cj} = V_i V_j |Y_S| \cos(\delta_s + \theta_j - \theta_i) - V_j^2 |Y_S| \cos\delta_s \quad (17)$$

$$Q_{cj} = V_i V_j |Y_S| \sin(\delta_s + \theta_j - \theta_i) - V_j^2 |Y_S| \sin\delta_s + Y_C V_j^2 \quad (18)$$

Using equations (15) - (18) the Jacobian matrix J form in equation (3) is modified to reflect the effects of the active and reactive power injections at buses i and j. Totally 16 elements need to be modified, and they are combined together to form the matrix ΔJ :

$$\Delta J = \begin{bmatrix} \Delta\frac{\partial P_i}{\partial\theta_i} & \Delta\frac{\partial P_i}{\partial\theta_j} & \Delta\frac{\partial P_i}{\partial V_i} & \Delta\frac{\partial P_i}{\partial V_j} \\ \Delta\frac{\partial P_j}{\partial\theta_i} & \Delta\frac{\partial P_j}{\partial\theta_j} & \Delta\frac{\partial P_j}{\partial V_i} & \Delta\frac{\partial P_j}{\partial V_j} \\ \Delta\frac{\partial Q_i}{\partial\theta_i} & \Delta\frac{\partial Q_i}{\partial\theta_j} & \Delta\frac{\partial Q_i}{\partial V_i} & \Delta\frac{\partial Q_i}{\partial V_j} \\ \Delta\frac{\partial Q_j}{\partial\theta_i} & \Delta\frac{\partial Q_j}{\partial\theta_j} & \Delta\frac{\partial Q_j}{\partial V_i} & \Delta\frac{\partial Q_j}{\partial V_j} \end{bmatrix} \quad (19)$$

The elements of ΔJ (which are listed in [21]) should be added to their corresponding positions in the original J . This process is represented in matrix form as follows:

$$J' = J + M\,\Delta J M^{t} \qquad (20)$$

where M has the following form:

$$M = \begin{bmatrix} N & | & 0 \\ -- & | & -- \\ 0 & | & N \end{bmatrix} \qquad (21)$$

where 0 **:** is $n \times 2$ zero matrix

N **:** sparse Matrix in the form $N = \begin{bmatrix} e_i & e_j \end{bmatrix}$

e_i, e_j **:** spares column vectors with only one unity element at position *i* and j respectively.

The voltage stability index VSI is used in this paper in contingency ranking [22]. VSI can be defined by:

$$VSI_{ij} = \frac{4 Z_{ij}^{2} Q_j}{V_i^{2} X_{ij}}$$

where Z_{ij} is the line impedance, Q_j is the reactive power at the receiving bus, V_i is the voltage at the sending bus, X_{ij} is the line reactance between buses *i* and *j*.

The computation procedures will be as following:

1- Base load flow computation is done .
2- Short listing of possible line outage contingencies is selected(this is done by reviewing the critical lines for the same studied system in the literatures)
3- Line outage contingencies is simulated by removing each line at a time.
4- VSI values are computed for each line for all selected contingencies.
5- The highest VSI value from every line outages are ranked and the line outage with highest rank is identified as the most critical outage .

In the following section, modeling of FACTS devices used in this paper are presented.

4. MODELING OF PROPOSED SYSTEM WITH STATCOM AND SSSC

There are many models used to represent STATCOM and SSSC devices. The most suitable models for steady state voltage stability studies are presented in the following sections.

4.1 Modeling of STATCOM Controller

A schematic representation of the one-phase STATCOM is shown in Fig.2. It is composed of a voltage source converter (VSC) connected on the secondary side of a coupling transformer. The VSC uses forced commuted power electronics devices (GTO's or IGBT's) to synthesize the voltage from a dc voltage source. The capacitor connected on the DC side of the VSC acts as a dc voltage source.

To explain the basic STATCOM operation principles, its equivalent circuit is depicted in Fig.3 , where V_{sh} represents the voltage in the STATCOM terminals and V_i is the voltage on bus i. It is considered that the coupling transformer is lossless.

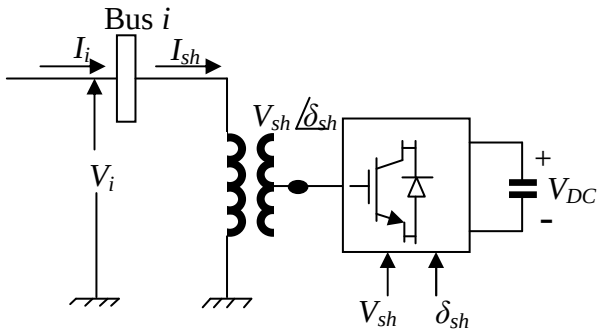

Fig. 2: Schematic diagram of STATCOM at Bus

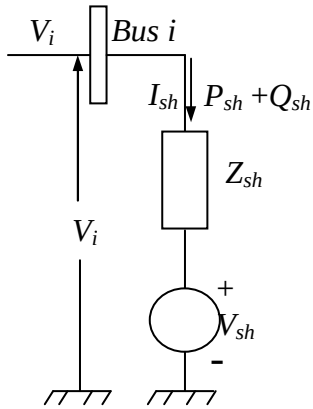

Fig. 3: STATCOM equivalent circuit

According to the equivalent circuit of the STATCOM shown in Fig.3, let:

$$V_{sh} = V_{sh}\angle\theta_{sh} \ , \quad V_i = V_i\angle\theta_i$$

So the STATCOM power flow constraints should be:

$$P_{sh} = V_i^2 g_{sh} - V_i V_{sh}(g_{sh}\cos(\theta_i - \theta_{sh}) + b_{sh}\sin(\theta_i - \theta_{sh})) \qquad (22)$$

$$Q_{sh} = -V_i^2 b_{sh} - V_i V_{sh}(g_{sh}\sin(\theta_i - \theta_{sh}) - b_{sh}\cos(\theta_i - \theta_{sh})) \qquad (23)$$

where $Y_{sh}=1/Z_{sh} = g_{sh} + jb_{sh}$.

Operating constraint of the STATCOM – the active power exchange via the DC link is zero, which is described by :

$$PE = \mathrm{Re}(V_{sh} I_{sh}^{*}) = 0 \qquad (24)$$

where ,

$$\mathrm{Re}(V_{sh} I_{sh}^{*}) = V_{sh}^{2} g_{sh} - V_i V_{sh} (g_{sh} \cos(\theta_i - \theta_{sh}) - b_{sh} \sin(\theta_i - \theta_{sh}))$$

The bus voltage control mode is used to improve the voltage stability so the bus voltage control constraint is given by :

$$\Delta F = V_i - V_i^{sp} = 0 \qquad (25)$$

where V_i^{sp} is the bus voltage control reference.

After inserting the STATCOM, the power flow relationship is modified to be:

$$\begin{bmatrix} -\Delta P_h \\ -\Delta Q_h \\ \cdots\cdots \\ -\Delta PE \\ -\Delta F \end{bmatrix} = \begin{bmatrix} \frac{\partial P_h^{new}}{\partial \theta_h} & \frac{\partial P_h^{new}}{\partial V_h} & \vdots & \frac{\partial P_h}{\partial V_{sh}} & \frac{\partial P_h}{\partial \theta_{sh}} \\ \frac{\partial Q_h^{new}}{\partial \theta_h} & \frac{\partial Q_h^{new}}{\partial V_h} & \vdots & \frac{\partial Q_h}{\partial V_{sh}} & \frac{\partial Q_h}{\partial \theta_{sh}} \\ \cdots\cdots & \cdots\cdots & \vdots & \cdots\cdots & \cdots\cdots \\ \frac{\partial PE}{\partial \theta_h} & \frac{\partial PE}{\partial V_h} & \vdots & \frac{\partial PE}{\partial V_{sh}} & \frac{\partial PE}{\partial \theta_{sh}} \\ \frac{\partial F}{\partial \theta_h} & \frac{\partial F}{\partial V_h} & \vdots & \frac{\partial F}{\partial V_{sh}} & \frac{\partial F}{\partial \theta_{sh}} \end{bmatrix} \begin{bmatrix} \Delta \theta_h \\ \Delta V_h \\ \cdots\cdots \\ \Delta V_{sh} \\ \Delta \theta_{sh} \end{bmatrix} \qquad (26)$$

where $h = i,j,\ldots$

4.2 Modeling of SSSC Controller

A SSSC basically consists of a series coupling transformer, a solid-state voltage source converter with several gate turn off (GTO) thyristor switch-based valves and a capacitor. The schematic diagram of the basic structure of SSSC inserted between two buses is shown in Fig.4.

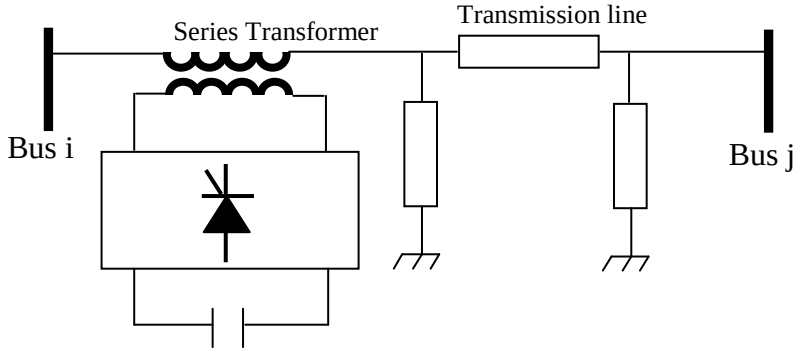

Fig. 4: Schematic diagram of SSSC between Bus i and Bus j

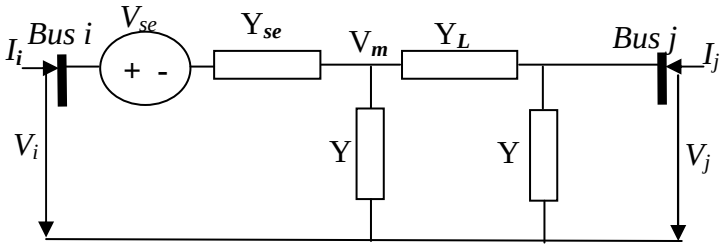

Fig. 5. SSSC equivalent circuit

To develop the SSSC model its equivalent circuit with two port pi-model of the transmission line is presented in Fig.5. Where the converter is represented by voltage source with series impedance (admittance). In this circuit, $V_i = V_i \angle \theta_i$ and $V_j = V_j \angle \theta_j$ are the voltages at bus *i* and *j*. $V_{se} = V_{se} \angle \theta_{se}$ is the series injected voltage of SSSC. $Y_{se} = G_{se} + jB_{se}$ and $Z_{se} = R_{se} + jX_{se}$ is the admittance and impedance of series coupling transformer. $Y = jB$ and $Y_L = G_L + jB_L$ are the charging susceptance and admittance of the transmission line respectively. From Fig.5 the following relations hold:

$$\begin{bmatrix} V_i \\ I_i \end{bmatrix} = \begin{bmatrix} 1 & Z_{se} \\ 0 & 1 \end{bmatrix} \begin{bmatrix} V_m \\ I_m \end{bmatrix} + \begin{bmatrix} 1 \\ 0 \end{bmatrix} V_{se} \qquad (27)$$

The two port network of pi-model of transmission line is described by the following equation:

$$\begin{bmatrix} I_m \\ I_j \end{bmatrix} = \begin{bmatrix} Y + Y_L & -Y_L \\ -Y_L & Y + Y_L \end{bmatrix} \begin{bmatrix} V_m \\ V_j \end{bmatrix} \qquad (28)$$

where $I_m = I_i$

From SSSC part of the circuit:

$$V_m = V_i + V_{se} - (1/Y_{se}) I_i \qquad (29)$$

By substituting V_m from equation (29) into equation (28):

$$I_i = Y_{ii} V_i + Y_{ij} V_j + Y_{bi} V_{se} \qquad (30)$$

where,

$$Y_{ii} = G_{ii} + jB_{ii} = (Y_{se}Y_L + Y_{se}Y)/Y_T$$
$$Y_T = Y_{se} + Y + Y_L$$
$$Y_{ij} = G_{ij} + jB_{ij} = -Y_{se}Y_L/Y_T$$
$$Y_{bi} = G_{bi} + jB_{bi} = Y_{se}(Y_L + Y)/Y_T$$

Also, from equation (30) and equation (28) we have:

$$I_j = Y_{ji}V_i + Y_{jj}V_j + Y_{bj}V_{se} \quad (31)$$

where,

$$Y_{jj} = G_{jj} + jB_{jj} = (Y_{se}Y_L/Y_T) + Y(Y_{se} + 2Y_L + Y)/Y_T$$
$$Y_{ji} = Y_{ij}$$
$$Y_{bj} = G_{bj} + jB_{bj} = -Y_{se}Y_L/Y_T$$

So the active, and reactive power of *i* and *j* buses after inserting the SSSC will be as follows:

$$P_i^{ss} = V_i^2 G_{ii} + V_i V_j \left[G_{ij}\cos(\theta_i - \theta_j) + B_{ij}\sin(\theta_i - \theta_j)\right] + V_i V_{se}\left[G_{bi}\cos(\theta_i - \theta_{se}) + B_{bi}\sin(\theta_i - \theta_{se})\right] \quad (32)$$

$$Q_i^{ss} = -V_i^2 B_{ii} + V_i V_j \left[G_{ij}\sin(\theta_i - \theta_j) - B_{ij}\cos(\theta_i - \theta_j)\right] + V_i V_{se}\left[G_{bi}\sin(\theta_i - \theta_{se}) - B_{bi}\cos(\theta_i - \theta_{se})\right] \quad (33)$$

$$P_j^{ss} = V_j^2 G_{jj} + V_i V_j \left[G_{ij}\cos(\theta_j - \theta_i) + B_{ij}\sin(\theta_j - \theta_i)\right] + V_j V_{se}\left[G_{bj}\cos(\theta_j - \theta_{se}) + B_{bj}\sin(\theta_j - \theta_{se})\right] \quad (34)$$

$$Q_j^{ss} = -V_j^2 B_{jj} + V_i V_j \left[G_{ij}\sin(\theta_j - \theta_i) - B_{ij}\cos(\theta_j - \theta_i)\right] + V_j V_{se}\left[G_{bj}\sin(\theta_j - \theta_{se}) - B_{bj}\cos(\theta_j - \theta_{se})\right] \quad (35)$$

The operating constraint of the SSSC (the active power exchange via the dc link) is:

$$PE = \mathrm{Re}(V_{se}I_i^*) = 0 \quad (37)$$

where

$$\mathrm{Re}(V_{se} I_i^*) = V_{se}^2 G_{bi} + V_{se} V_i \left[G_{ii} \cos(\theta_{se} - \theta_i) + B_{ii} \sin(\theta_{se} - \theta_i) \right] + V_{se} V_j \left[G_{ij} \cos(\theta_{se} - \theta_j) + B_{ij} \sin(\theta_{se} - \theta_j) \right]$$

In the practical applications of the SSSC, it may be used for control of one of the following parameters: 1) the active power flow of the transmission line, 2) the reactive power flow of the transmission line, 3) the bus voltage, and 4) the impedance of the transmission line. Therefore, the SSSC may have four control modes [23]. Among the four control modes, the bus voltage control mode is used here to improve the voltage stability so the bus voltage control constraint is given by:

$$\Delta F = V_i - V_i^{sp} = 0 \tag{38}$$

where V_i^{sp} is the bus voltage control reference

To implement the SSSC in Newton-Raphson power flow, the power mismatches equations will be:

$$\Delta P_h = P_{gh} - P_{dh} - P_h = 0$$
$$\Delta Q_h = Q_{gh} - Q_{dh} - Q_h = 0 \tag{39}$$

where,

- P_h and Q_h are, respectively, the real and reactive power leaving the bus-*h (h=i,j,…).*
- P_{gh} and Q_{gh} are, respectively, the real and reactive power entering the bus-*h (h=i,j,…).*
- P_{dh} and Q_{dh} are, respectively, the real and reactive load demand at bus-*h (h=i,j,…).*

The Newton-Raphson algorithm is expressed by the following relationship:

$$\begin{bmatrix} -\Delta P_h \\ -\Delta Q_h \end{bmatrix} = \begin{bmatrix} \frac{\partial P_h}{\partial \theta_h} & \frac{\partial P_h}{\partial V_h} \\ \frac{\partial Q_h}{\partial \theta_h} & \frac{\partial Q_h}{\partial V_h} \end{bmatrix} \begin{bmatrix} \Delta \theta_h \\ \Delta V_h \end{bmatrix} \tag{40}$$

After inserting the SSSC, the power flow relationship is modified to be:

$$\begin{bmatrix} -\Delta P_h \\ -\Delta Q_h \\ \cdots\cdots\cdots \\ -\Delta PE \\ -\Delta F \end{bmatrix} = \begin{bmatrix} \frac{\partial P_h^{new}}{\partial \theta_h} & \frac{\partial P_h^{new}}{\partial V_h} & \vdots & \frac{\partial P_h}{\partial V_{se}} & \frac{\partial P_h}{\partial \theta_{se}} \\ \frac{\partial Q_h^{new}}{\partial \theta_h} & \frac{\partial Q_h^{new}}{\partial V_h} & \vdots & \frac{\partial Q_h}{\partial V_{se}} & \frac{\partial Q_h}{\partial \theta_{se}} \\ \cdots\cdots & \cdots\cdots & \vdots & \cdots\cdots & \cdots\cdots \\ \frac{\partial PE}{\partial \theta_h} & \frac{\partial PE}{\partial V_h} & \vdots & \frac{\partial PE}{\partial V_{se}} & \frac{\partial PE}{\partial \theta_{se}} \\ \frac{\partial F}{\partial \theta_h} & \frac{\partial F}{\partial V_h} & \vdots & \frac{\partial F}{\partial V_{se}} & \frac{\partial F}{\partial \theta_{se}} \end{bmatrix} \begin{bmatrix} \Delta\theta_h \\ \Delta V_h \\ \cdots\cdots\cdots \\ \Delta V_{se} \\ \Delta\theta_{se} \end{bmatrix} \qquad (41)$$

where, $\frac{\partial F}{\partial \theta_h}, \left(\frac{\partial F}{\partial V_h}\right)_{h\neq i}, \frac{\partial F}{\partial V_{se}}$, *and* $\frac{\partial F}{\partial \theta_{se}}$ *equal zero. and* $\frac{\partial F}{\partial V_i} = 1$

The modified Jacobian matrix is split into four blocks by the dotted line, the upper diagonal block has the same structure as that of the system Jacobian matrix of conventional power flow [23] though the terms of former should consider the contributions from the SSSC. The other three blocks of the Jacobian matrix are SSSC related. The superscripts new are used to indicate the contribution of SSSC for buses i , j for these buses:

$$\frac{\partial P_h^{new}}{\partial \theta_h} = \frac{\partial P_h}{\partial \theta_h} + \frac{\partial P_h^{ss}}{\partial \theta_h} \quad , \quad \frac{\partial P_h^{new}}{\partial V_h} = \frac{\partial P_h}{\partial V_h} + \frac{\partial P_h^{ss}}{\partial V_h}$$

$$\frac{\partial Q_h^{new}}{\partial \theta_h} = \frac{\partial Q_h}{\partial \theta_h} + \frac{\partial Q_h^{ss}}{\partial \theta_h} \quad , \quad \frac{\partial Q_h^{new}}{\partial V_h} = \frac{\partial Q_h}{\partial V_h} + \frac{\partial Q_h^{ss}}{\partial V_h}$$

5. SIMULATION RESULTS

Voltage stability enhancement using the proposed FACTS devices is done through the simulation of IEEE 30- bus test system (shown in Fig.6). Studied system data is obtained from reference [24]. All the results are produced by programs developed in MATLAB® software package.

The system consists of 6 machines ,30 buses, and 41 lines. Bus 1 is considered as slack bus, while 5 nodes as PV buses and other buses as PQ buses. For all cases, the convergence tolerance is 1e-12 p.u. and system base is 100 MVA

As explained in the previous sections the best location of the STATCOM is done by modal analysis, while voltage stability index is used for identifying the best location of the SSSC.

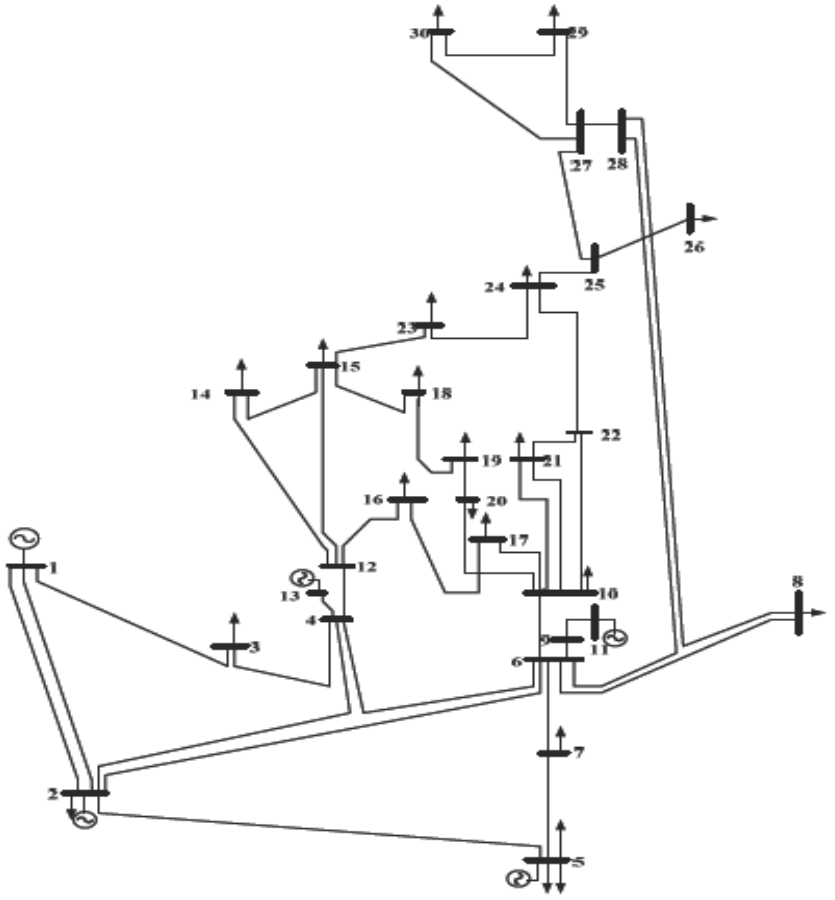

Fig. 6 The IEEE 30-bus power system

5.1 Identification of the Weakest Bus

The modal analysis method is applied to the suggested test systems. The voltage profile of the buses is presented from the load flow simulation. Then, the minimum eigenvalue of the reduced Jacobian matrix is calculated. After that, the weakest load buses, which are subject to voltage collapse, are identified by computing the participating factors. The results are shown in Fig. 7, Fig. 8, and Table 1.

Figure 7 shows the voltage profile of all buses of the IEEE 30 Bus system as obtained from the load flow. It can be seen that all the bus voltages are within the acceptable level (□□5%) except bus number 30, which is about 0.944 p.u.

The total number of eigenvalues of the reduced Jacobian matrix *JR* is 24, as there are 24 PQ buses. These eigenvalues are shown in Table 1. All the eigenvalues are positive which means that the system voltage is stable. It can be noticed that the minimum eigenvalue that equal to 0.513 is the most critical mode. The participating factor for this mode has been calculated and the result is shown in Fig. 8. The results

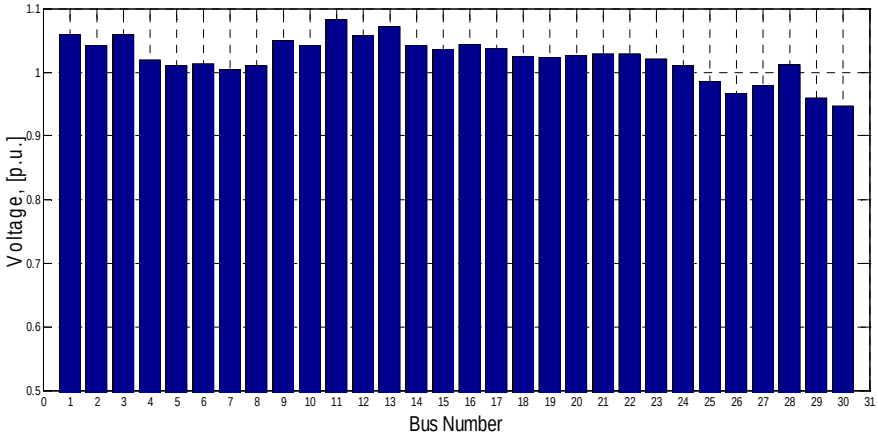

Fig.7: Voltage profile for all buses without FACTS

Table 1: The eigen values for the studied power system

Bus No.	Eigenvalue	Bus No.	Eigenvalue
1	107.48766	13	18.72292
2	100.92729	14	3.59637
3	59.71765	15	4.06940
4	47.33923	16	5.48372
5	37.90579	17	6.04582
6	34.85240	18	16.44144
7	23.35048	19	15.58759
8	22.81107	20	12.90193
9	0.51305	21	13.69709
10	1.03581	22	8.82146
11	1.73317	23	7.48722
12	19.83127	24	5.69517

show that, the buses 30, 29 and 26 have the highest participation factors for the critical mode. The largest participation factor value (0.22) at bus 30 indicates the highest contribution of this bus to the voltage collapse.

The Q-V curves are depicted in Fig. 9 for the weakest buses of the critical mode as expected by the modal analysis method. The curve verifies the results obtained previously by modal analysis method. It can be seen that buses 30, and 26 are the critical buses compared with the bus 29 but with keeping in mind the participation factors of the bus 30 will be the most critical one, where any more increase in the reactive power demand in that bus will cause a voltage collapse. Therefore Bus 30 is selected to place STATCOM FACTS device at it.

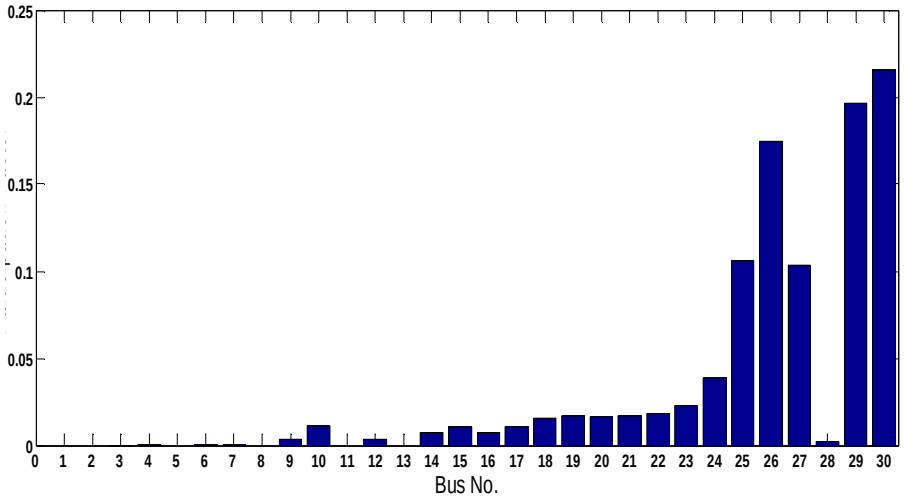

Fig.8: Participation factors for load buses

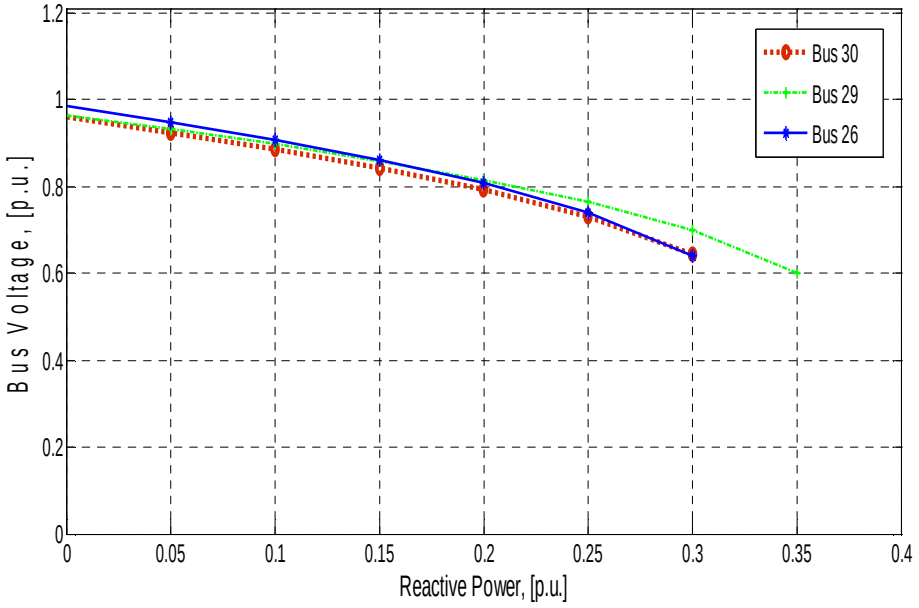

Fig.9: Q-V curves for critical buses

5.2 Critical Line for SSSC Placement

To define the suitable placement of SSSC, firstly the line outage is simulated then the VSI are computed as in section 3.2. From the values of VSI under line outage contingencies listed in Table 2 it is clearly seen that at line L38 (the line connecting buses 27-30) outage all the buses have the highest VSI . furthermore L38 itself has the

highest VSI value under all the selected contingencies. The line L39 has the second highest VSI value. These results are expected since the two lines are connected to the weakest bus number 30 which is identified by the model analysis. So, the line L38 is chosen to place SSSC device.

5.3 Simulation Results With Effect of STATCOM and SSSC

To investigate the effect of the STATCOM device, PV curves of the critical buses 26, 29, and 30 without and with STATCOM are depicted in Fig.10 to Fig. 12. In Fig. 10 the voltage of bus 30 (where the STATCOM is placed) is fixed at the targeted value of 1 pu. despite the increasing of the loading factor to 1.4. Also, in Fig. 11 and Fig. 12 the voltages are more closely to the nominal values. So, all the results show that the voltage profiles are enhanced and consequently the voltage stability margin of the studied system is improved due to the use of STATCOM.

The cases of using SSSC (at line 27-30) are shown in Fig. 13 to Fig. 15 , as in STATCOM, the SSSC improves the voltage profiles for critical buses. Fig. 13 indicates that the device succeeds to fix the voltage of the most critical bus 30 to the objective value. Fig. 14 shows an improvement in the voltage profiles of buses 29.

In Fig. 15, the voltage profile before and after SSSC connected is nearly unchanged. To explore the reason, a first glance to the studied system in Fig. 6 indicates that, bus 26 is not connected neither to bus 30 nor bus 27. So the effect of SSSC (put in the line 27-30) on bus 26 is very small.

The voltage profile snapshot of all buses with the different proposed FACTS is shown in Fig. 16. It is noticed that all the buses voltages are kept within the acceptable range. While the voltage magnitudes of all buses using STATCOM are greater than the magnitudes obtained using SSSC.

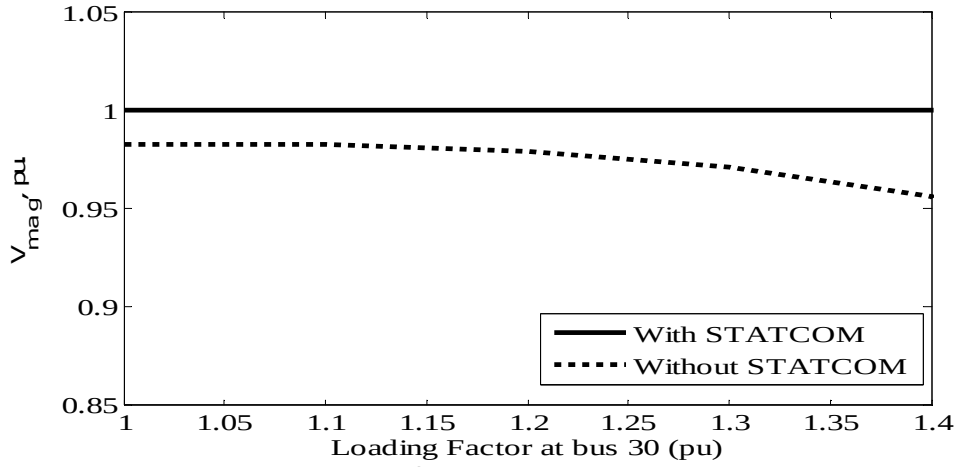

Fig.10 P-V curve of bus 30 with and with out STATCOM

Table 2. VSI for the studied power system under different lines outage

Line No	Line outage									
	L13	**L16**	**L21**	**L24**	**L29**	**L31**	**L32**	**L33**	**L38**	**L39**
L1(1-2)	0.028	0.027	0.104	0.242	0.325	0.370	0.418	0.468	0.999	0.999
L2(1-3)	0.062	0.254	0.648	0.999	0.999	0.999	0.999	0.999	0.999	0.430
L3(2-4)	0.154	0.440	0.999	0.999	0.999	0.999	0.999	0.999	0.999	0.999
L4(3-4)	0.035	0.101	0.251	0.399	0.518	0.583	0.654	0.720	0.999	0.999
L5(2-5)	0.999	0.999	0.999	0.999	0.999	0.999	0.999	0.999	0.999	0.999
L6(2-6)	0.144	0.350	0.723	0.999	0.999	0.999	0.999	0.999	0.999	0.999
L7(4-6)	0.035	0.085	0.177	0.314	0.403	0.457	0.506	0.547	0.999	0.999
L8(5-7)	0.796	0.999	0.999	0.999	0.999	0.999	0.999	0.999	0.999	0.999
L9(6-7)	0.533	0.999	0.999	0.999	0.999	0.999	0.999	0.999	0.999	0.999
L10(6-8)	0.497	0.999	0.999	0.999	0.999	0.999	0.999	0.999	0.999	0.999
L11(6-9)	0.296	0.000	0.000	0.000	0.000	0.000	0.000	0.000	0.999	0.999
L12(6-10)	0.999	0.999	0.999	0.999	0.999	0.999	0.999	0.999	0.999	0.999
L13(9-11)	0.043	0.593	0.999	0.999	0.999	0.999	0.999	0.999	0.999	0.999
L14(9-10)	0.999	0.999	0.999	0.999	0.999	0.999	0.999	0.999	0.999	0.999
L15(4-12)	0.999	0.999	0.999	0.999	0.999	0.999	0.999	0.999	0.999	0.999
L16(12-13)	0.146	0.309	0.893	0.000	0.999	0.999	0.999	0.999	0.999	0.999
L17(12-14)	0.700	0.999	0.999	0.999	0.999	0.999	0.999	0.999	0.999	0.999
L18(12-15)	0.302	0.588	0.999	0.999	0.999	0.999	0.999	0.999	0.999	0.999
L19(12-16)	0.169	0.325	0.454	0.880	0.999	0.999	0.999	0.999	0.999	0.999
L20(14-15)	0.846	0.999	0.999	0.999	0.999	0.999	0.999	0.999	0.999	0.999
L21(16-17)	0.495	0.953	0.999	0.999	0.999	0.999	0.999	0.999	0.999	0.999
L22(15-18)	0.277	0.541	0.999	0.999	0.999	0.999	0.999	0.999	0.999	0.999
L23(18-19)	0.462	0895	0.999	0.999	0.999	0.999	0.999	0.999	0.999	0.999
L24(19-20)	0.076	0.149	0.287	0.394	0.513	0.566	0.624	0.680	0.999	0.999
L25(10-20)	0.217	0.427	0.822	0.999	0.999	0.999	0.999	0.999	0.999	0.999
L26(10-17)	0.214	0.413	0.823	0.999	0.999	0.999	0.999	0.999	0.999	0.999
L27(10-21)	0.353	0.672	0.999	0.999	0.999	0.999	0.999	0.999	0.999	0.999
L28(10-22)	0.074	0.152	0.305	0.434	0.541	0.592	0.601	0.696	0.999	0.999
L29(21-23)	0.023	0.045	0.085	0.122	0.132	0.166	0.028	0.198	0.999	0.999
L30(15-23)	0.195	0.375	0.707	0.999	0.999	0.999	0.229	0.999	0.999	0.999
L31(22-24)	0.270	0.477	0.826	0.999	0.999	0.999	0.999	0.999	0.999	0.999
L32(23-24)	0.359	0.635	0.999	0.999	0.999	0.999	0.999	0.999	0.999	0.999
L33(24-25)	0.123	0.247	0476	0.711	0.886	0.965	0.999	0.999	0.999	0.999
L34(25-26)	0.241	0.429	0.756	0.999	0.999	0.999	0.999	0.999	0.999	0.445
L35(25-27)	0.999	0.949	0.999	0.999	0.999	0.999	0.999	0.999	0.999	0.999
L36(28-27)	0.999	0.999	0.999	0.912	0.999	0.999	0.999	0.999	0.999	0.999
L37(27-29)	0.360	0.693	0.999	0.999	0.999	0.999	0.999	0.999	0.999	0.999
L38(27-30)	0.999	0.999	0.999	0.999	0.999	0.999	0.999	0.999	0.999	0.999
L39(29-30)	0.999	0.999	0.999	0.999	0.999	0.999	0.999	0.999	0.999	0.999
L40(8-28)	0.109	0.261	0.542	0.894	0.999	0.999	0.999	0.999	0.999	0.546
L41(6-28)	0.032	0.077	0.159	0.265	0.338	0.360	0.398	0.505	0.999	0.999

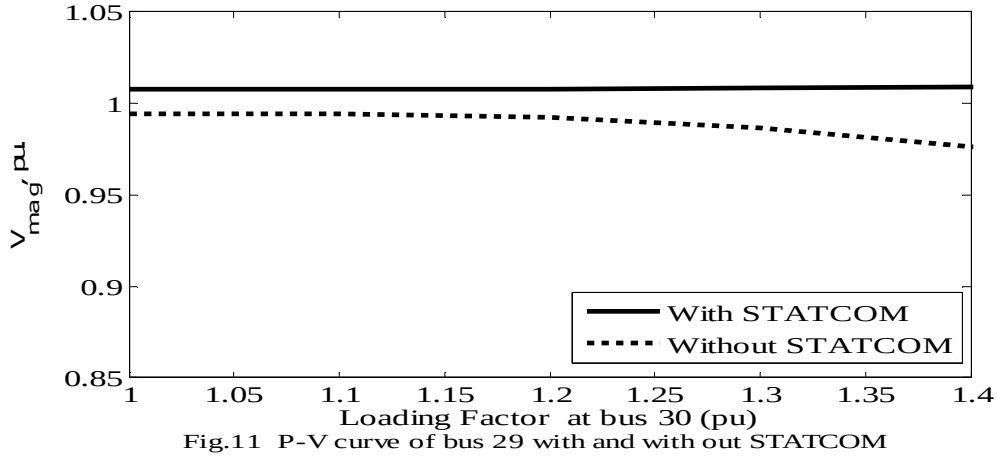

Fig.11 P-V curve of bus 29 with and with out STATCOM

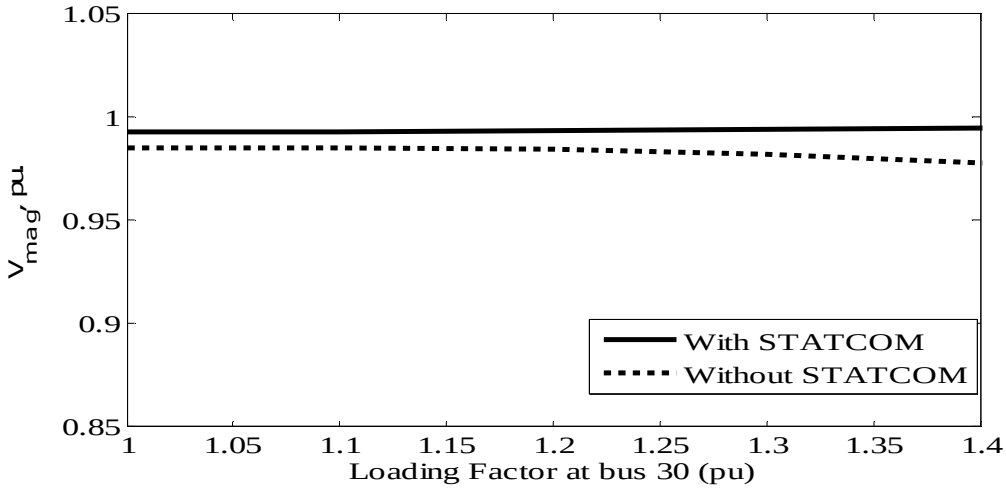

Fig.12 P-V curve of bus 26 with and with out STATCOM

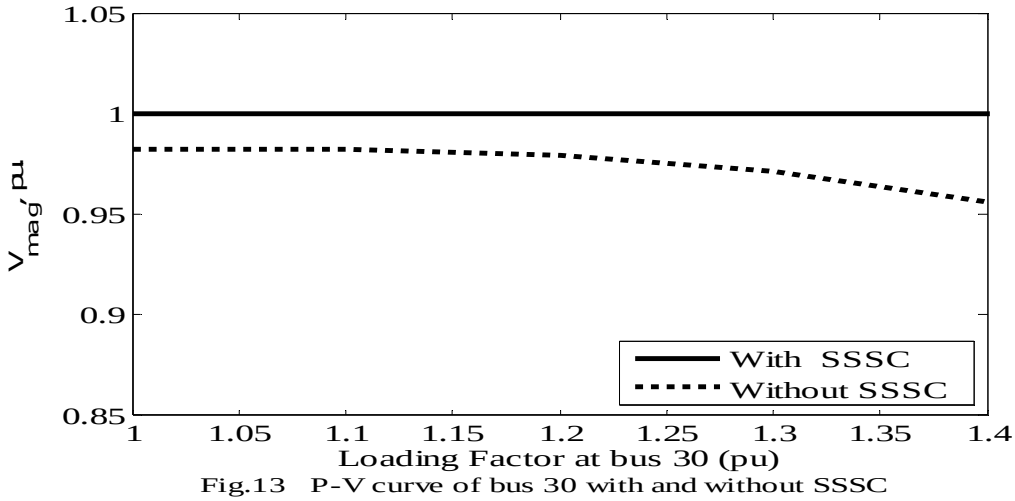

Fig.13 P-V curve of bus 30 with and without SSSC

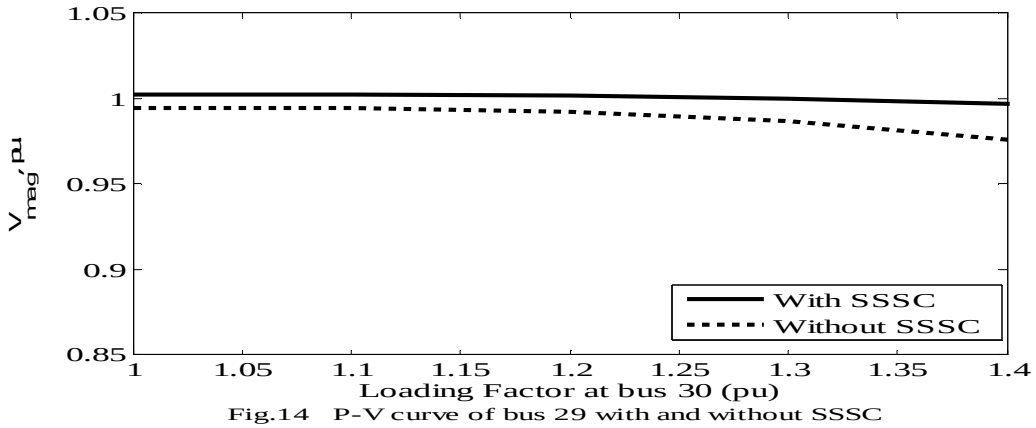

Fig.14 P-V curve of bus 29 with and without SSSC

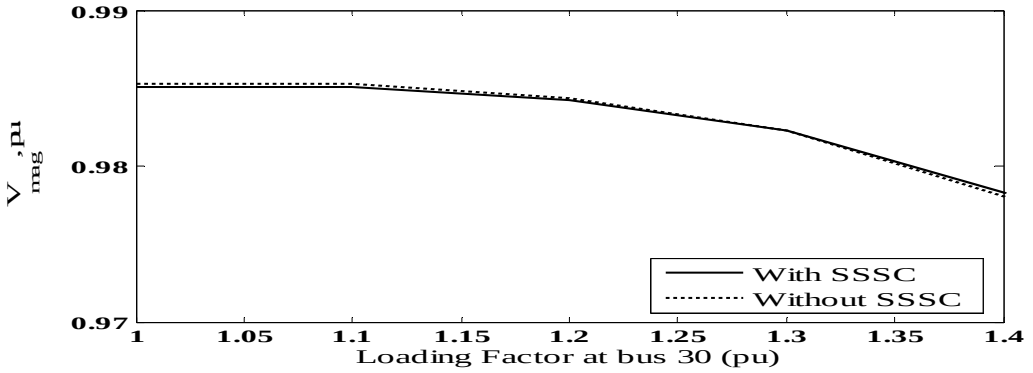

Fig.15 P-V curve of bus 26 with and without SSSC

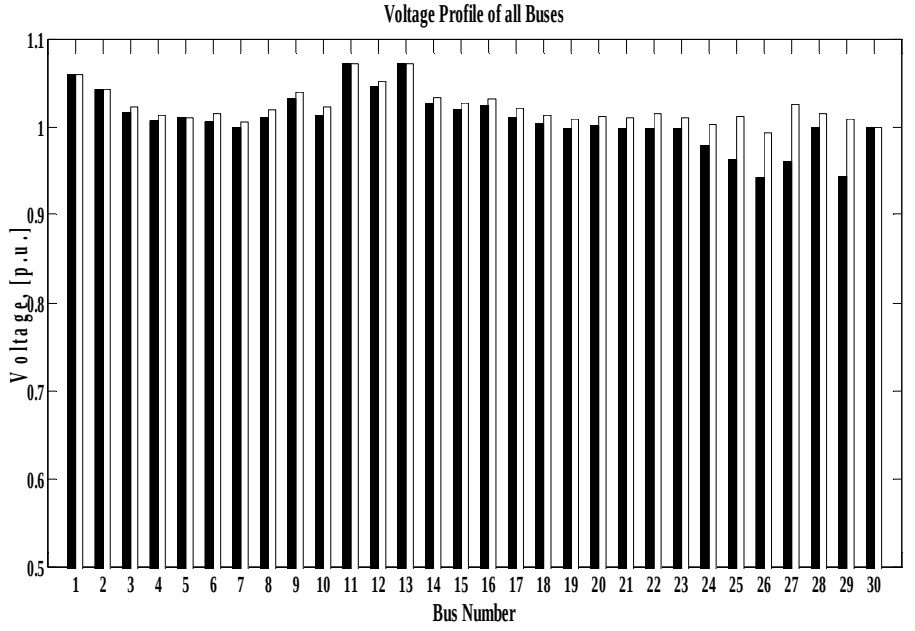

Fig. 16: Voltage profile for all buses with either STATCOM or SSSC

6. CONCLUSION

This paper introduces a study of the STATCOM and SSSC used for steady state voltage stability improvement. Detailed steady state models of both FACTS devices are presented focusing on the inclusion of these devices into the power flow analysis process. Two different algorithms suitable for best placement of the devices are proposed. These devices prove their ability to enhance voltage stability margin. The simulation results show that the insertion of STATCOM improves the voltage profiles and the system steady state stability of the studied system is better than that obtained with using SSSC device.

REFERENCES

[1] Ajjarapu V., Lee B., "Bibliography on voltage stability," IEEE Trans. Power Systems, Vol. 13, No. 1, Feb. 1998, pp. 115-125

[2] T.V Cutsem, "Voltage stability of electric power system", Springer, 1998

[3] IEEE/CIGRE Joint Task Force on Stability Terms and Definitions, "Definition and classification of power system stability," IEEE Transactions on Power Systems, Vol. 19, No. 2, pp. 1387–1401, May 2004.

[4] S. Gupta, R.K Tripathi, R.D. Shukla, D. Povh, K. Renz, E. Teltsch, and R.Witzmann, "Voltage stability improvement in power systems using facts controllers: State-of-the-art review," Proceedings of International Conference on Power, Control and Embedded Systems (ICPCES), Allahabad, India, Nov. 2010, pp. 1-8.

[5] Xiaohua Huang, Guomin Zhang, and Liye Xiao, "Optimal location of SMES for improving power system voltage stability," IEEE Transactions on Applied Superconductivity, Vol. 20, No. 3, pp. 1316–1319, Jun. 1996.

[6] Baochun Lu, Baoguo Li, Yi Liu, Weiguo Guan, and Gang Lv, "Studies of voltage stability based on SVC control," Proceedings of 3rd International Conference on Innovative Computing Information and Control (ICICIC '08), Dalian, China, June. 2008, pp. 124-128.

[7] Ma You-jie, Liu Jin-hua, Zhou Xue-song, and Wen Hu-long, "The static bifurcation analysis of STATCOM on power system voltage stability," Proceedings of 3rd International Conference on Measuring Technology and Mechatronics Automation , (ICMTMA), Shanghai, China, Jan. 2011, pp. 953-957.

[8] M. Gitizadeh and M. Kalantar, "A new approach for optimal location of TCSC in a power system to enhance voltage stability: steady state studies," Proceedings of 42nd International Universities Power Engineering Conference (UPEC), Brighton, UK, Sep. 2007, pp. 953-957.

[9] M.Kowsalya, Kanika Garg, and Neha Gupta, "Series Compensation for Static and Dynamic Voltage Stability Enhancement," Proceedings of Conference on Innovative Technologies in Intelligent Systems and Industrial Applications (CITISIA), Sunway campus, Malaysia, July 2009, pp. 402-406.

[10] A. Karami , M. Rashidinejad, and A. A. Gharaveisi, " Voltage security enhancement and congestion management via STATCOM & IPFC using artificial intelligence," Iranian Journal of Science & Technology, Vol 31, No. 3, pp. 289–301, June 2007.

[11] J. Raju, and P.S. Venkataramu, "Effect of UPFC on Voltage Stability Margin," Proceedings of International Conference on Power System Technology (POWERCON 2008), New Delhi, India, Oct. 2008.

[12] M. A. Kamarposhti, M. Alinezhad, H. Lesani, and N. Talebi, "Comparison of SVC, STATCOM, TCSC, and UPFC controllers for Static Voltage Stability evaluated by continuation power flow method," Proceedings of The Electrical Power & Energy Conference (EPEC 2008), Vancouver, Canada, Oct. 2008.

[13] Arthit Sode-Yome, and N. Mithulananthan, "Comparison of shunt capacitor, SVC and STATCOM in static voltage stability margin enhancement," International Journal of Electrical Engineering Education, Vol. 41, No. 2, pp. 158–171, Apr. 2004.

[14] C. W. Taylor, "Power System Voltage Stability." New York: MaHraw-Hill, 1994.

[15] V. A. Venikov, V. A. Stroev, V. I. Idelchick, and V. I. Trasov, "Estimation of Electric Power System Steady-State Stability in Load Flow Calculation," IEEE Transactions on Power Apparatus and Systems, vol. PAS-94, pp. 1034-1041, May/June 1975.

[16] J. C. Chow, R. Fischl, and H. Yan, " on the evaluation of voltage collapse criteria" IEEE Transactions On Power Systems, Vol. 5, pp. 612-620, May 1990.

[17] A. Sode-Yome, N. Mithulananthan, K.Y. Lee, " A Comprehensive Comparison of FACTS Devices for Enhancing Static Voltage Stability," IEEE Power Engineering Society General Meeting, 2007, Florida, USA, June 2007, pp. 1-8.

[18] A. Al-Hinai and M. Choudhry "Voltage Collapse Prediction for Interconnected Power System", Proceedings of 33rd North American Power Symposium (NAPS), College Station, TX, Oct. 2001.

[19] B. Gao, G.K Morison and P. Kundur, "Voltage Stability Evaluation using Modal Analysis", IEEE Transactions on Power Systems, Vol. 7, No. 4, pp. 1529- 1542, Nov. 1992.

[20] K.L. Lo and Z.J. Meng, "Newton-like method for line outage simulation," IEE Proc. C Gener. Trans. Distrib., Vol. 151, No.2, pp. 225-231, March 2004.

[21] G.B. Jasmon, and C.Y. Chuan, "Performance comparison of two exact outage simulation techniques", IEE Proc. C Gener. Trans. Distrib., Vol. 132, No.6, pp. 285–293. Nov. 1985.

[22] Musirin and T. K. A. Rahman, "Estimating Maximum Loadability for Weak Bus Identification Using FVSI", IEEE Power Engineering Review, Vol. 22, 2002, pp. 50– 52, Nov. 2002.

[23] Xiao-Ping Zhang, "Advanced Modeling of the Multicontrol Functional Static Synchronous Series Compensator (SSSC) in Newton Power Flow," IEEE Transactions on Power Systems, Vol. 18, No. 4, pp. 1410–1416, Nov. 2003.

[24] Power System Test Case Archive: [Online] http://www.ee.washington.edu/ .

استخدام أجهزة أنظمة النقل المرنة ذات التيار المتناوب في تحسين استقرار الجهود لمنظومات القوى الكهربائية

تهدف هذه الدراسة لبحث تحسينالاستقرار (الاتزان) الاستاتيكي للجهود باستخدام نوعين من أجهزة أنظمة النقل المرنة ذات التيار المتناوب حيث تم استخدام " المعوض المتزامن الاستاتيكى " كجهاز يركب على التوازي وكذلك جهاز " المعوض المتزامن الاستاتيكى المتوالي " المركب على التوالي.

كخطوة أولية في البحث تم استخدام طريقة "التحليل المشروط" في تحديد أفضل نقطة في منظومة القدرة الكهربائية يمكن وضع جهاز التوازي عندها وذلك بهدف تحقيق أفضل تحسين ممكن لاتزان جهود المنظومة. كما تم استخدام طريقة جديدة تجمع ما بين " مؤشر الاقتراب من اتزان الجهد" وحالات خروج خطوط النقل من الخدمة لتحديد أكثر خطوط المنظومة ملائمةً لتركيب جهاز التوالي عليها.

ولاختبار أداء الأجهزة المذكورة ومدي مناسبة مواقعها المقترحة، تم استخدام المنظومة القياسية ذات الثلاثون قضيباً IEEE 30 bus ، ومثلت النتائج عند ظروف تحميل مختلفة ، وتم استعراض النتائج عند أكثر النقاط حساسية في المنظومة. وفي كل الأحوال أثبتت الأجهزة فعاليتها وحسن أدائها واستطاعتها تحسين جهود المنظومة. وعلاوة على ذلك أثبتت النتائج أن الجهاز المركب على التوازي أحسن أداءً – في مشكلة تحسين اتزان الجهود – من الجهاز المركب على التوالي.